Power-Based Droop Control in DC Microgrids Enabling Seamless Disconnection from AC Grids

Guangyuan Liu, Tommaso Caldognetto, Paolo Mattavelli
Dept. of Management and Engineering (DTG), University of Padova, Italy
Email: guangyuan.liu@studenti.unipd.it, tommaso.caldognetto@ieee.org, paolo.mattavelli@unipd.it

***Abstract*—This paper proposes a unified power-based droop control method for distributed energy resources in dc microgrids that can operate both in grid-connected and islanded mode. When the main grid is available, the bus voltage is regulated by the grid-interface ac/dc converter, while distributed energy resources operate as power controlled sources. During abnormal operation of the main grid (e.g., due to faults), the grid-interface converter loses the capability of regulating the bus voltage and the proposed controller inherently converts from a power controller to a droop controller, without any need of communication with other microgrid components, enabling the seamless transition between the two operating modes. The proposed solution is experimentally verified by a testbed having one grid-interface converter and four distributed energy resource converters, $5\,\mathrm{kW}$ of rated power each.**

***Index Terms*—dc microgrids; droop control; power regulation; seamless transition.**

I. Introduction

In recent years, distributed energy resources (DERs) such as distributed generators (DGs) based on renewable sources (e.g., photovoltaic, wind) and energy storage systems (ESSs) (e.g., batteries, super capacitors) have seen a widespread diffusion. An effective way to integrate different types of DERs and loads [1] in distribution grids is to aggregate them in the form of microgrids, which potentially improves energy management , conversion efficiency and grid reliability. DERs are typically interfaced with the distribution system by means of power electronic converters (PECs). Due to the intrinsic dc nature of the most of DERs and loads (e.g., electric vehicles, consumer electronics, LED lighting, etc.), there is a strong interest towards the development of dc microgrids [2]. Compared to their ac counterparts, dc microgrids can potentially achieve higher energy conversion efficiency and lower system costs, mainly by minimizing the number of dc/ac and ac/dc conversion stages. Moreover, dc operation removes any reactive power or frequency control issue, making the control easier and more effective [3].

The main control targets in dc microgrids are the regulation of the voltage of the distribution bus and of the powe r exchanged by DERs. To achieve these goals, several control approaches have been investigated recently. Among them, droop control is a popular decentralized solution to implement primary level control, where the bus voltage is employed to convey the loading condition of the microgrid. With traditional droop approaches, the droop curves of the grid-interface (GI) converter, the DGs and the ESSs are properly designed to obtain prioritized power management strategies [4], [5]. Fixed droop curves are often employed, which limit power control flexibility, making power contributions from DERs directly determined by loads power absorption. Moreover, distribution bus impedances strongly affect how the load is shared among sources, and the balance among battery systems with different state-of-charge (SoC) requires proper coordination between DGs and ESSs, which is only achieved by means of communication [6]. To address these issues, adjustable droop control methods have been proposed. By regulating to zero the difference between each converter's output current and the average output current, that is, by adjusting the droop coefficient and the voltage set point, the steady state mismatch current due to interconnecting impedances can be compensated [7], [8]. As for dynamic power sharing between batteries and super capacitors, frequency-based virtual impedances are implemented [9], [10]. As a result, batteries and super capacitors supply consistent power and high frequency power separately. To equalize SoC among multiple battery systems, the droop function of each battery system is modified according to its SoC [11], [12].

Extending [13] to dc microgrid, this paper proposes an alternative approach: during normal operation, DERs track the power references and the GI converter imposes bus voltage [14] and, during abnormal operation, DERs automatically switch, without any communication, to droop control, ensuring bus voltage regulation and DERs power sharing. The advantages of the proposed controller include *i)* regulation of DERs active power when the GI converter is operating normally, regardless of dc bus impedances, *ii)* regulation of the bus voltage with traditional droop control if the GI converter loses the capability of maintaining the bus voltage (e.g., due to power limitation or faults in the upstream grid), *iii)* smooth transitions between these two states, without using bus voltage variation detection schemes or communication with other components.

II. Control targets in dc microgrids

The layout of a typical dc microgrid is shown in Fig. 1. There are three major types of elements: GI, ESSs and DGs. The GI converter is used to interface the upstream ac grid with the dc network. ESSs are equipped with bidirectional dc/dc converters to allow charging and discharging of the energy

This work is partially supported by China Scholarship Council (CSC).

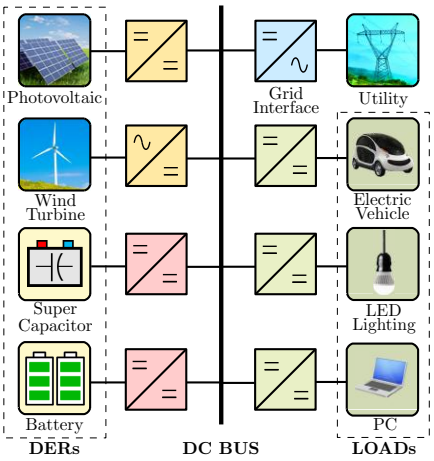

Figure 1. An example of dc microgrid layout.

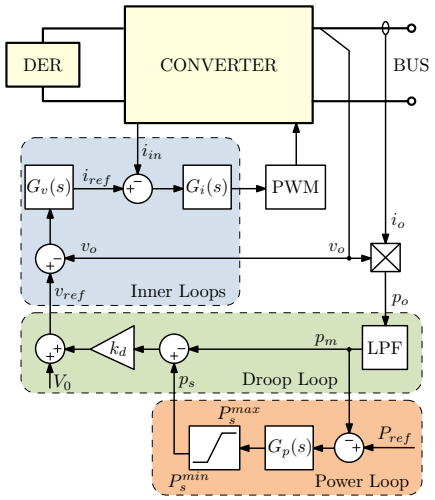

Figure 2. Scheme of the proposed control method.

storage units. DGs are connected to the microgrid by unidirectional converters (e.g., dc/dc converters for photovoltaic arrays, ac/dc converters for wind turbines). The proposed solution aims at two fundamental control objectives in the dc microgrid: regulating the dc bus voltage and regulating the power flow from DERs. These two goals cannot be achieved simultaneously by the same microgrid element; thus, each device operates pursuing only one specific goal at a time, and may switch to the other, as described hereafter.

1) GI: the GI converter regulates the bus voltage at a constant value and balances any power surplus or deficit in the dc microgrid. We denote this mode as *normal operation*. If the connection with the upstream grid is not available, for example due to faults of the main grid or due to GI converter power limitation, the GI converter is not able to regulate the bus voltage. We denote this mode as *abnormal operation*.

2) ESSs: during *normal operation*, ESSs are charged or discharged according to their SoC and grid energy management, operating as constant power sources. During *abnormal operation*, ESSs operate as droop-controlled sources to provide bus voltage regulation.

3) DGs: during *normal operation*, DGs track maximum power point (MPPT) to make full use of the local renewable source and they operate as constant power sources. During *abnormal operation*, there are two possible conditions: when the microgrid is heavily loaded, DGs continue to generate the power that maximizes the generation from the local renewable source; on the other hand, at light load, DGs do not follow the MPPT and take part in bus voltage regulation together with ESSs.

III. Concept of the Proposed Controller

In order to satisfy the aforementioned control targets, this paper presents a power-based droop control method for converters of ESSs and DGs. Fig. 2 shows the scheme of the proposed control approach, which mainly consists of three parts: inner voltage and current loops, droop loop and power loop.

1) Inner voltage and current loops: the inner voltage regulator $G_v(s)$ regulates the difference between the output voltage v_o and the voltage reference v_{ref} and generates the current reference i_{ref}. The current loop takes this current reference and the feedback of inner current i_{in} to produce the duty cycle.

2) Droop loop: the voltage-power droop control is adopted:

$$v_{ref} = (V_0 + k_d \cdot p_s) - k_d \cdot p_m \tag{1}$$

where v_{ref} is the ouput voltage reference, V_0 is the voltage set point, k_d is the droop coefficient, p_s is the offset determined by power loop and p_m is the measured output power. In traditional droop control, p_s should be zero. In our solution, it is utilized to shift the droop curve upwards or downwards. Moreover, a first-order low-pass filter with a cutoff frequency ω_c is used to measure the output power. It is worth mentioning that a voltage-current droop can be adopted as well.

3) Power loop: outside the droop loop, an external bounded power controller is added to track a given power reference P_{ref}. P_{ref} is determined by the microgrid supervisor using non-critical communication. $G_p(s)$ is employed to regulate the difference between P_{ref} and the measured power p_m. The variable offset p_s is generated by $G_p(s)$ to shift the droop curve, enabling power flow regulation. The upper and lower saturation levels of $G_p(s)$, P_s^{max} and P_s^{min} play a fundamental role in the controller. These two levels should be large enough to allow DERs to reach their nominal power. On the other hand, once the regulator $G_p(s)$ is saturated, the proposed controller becomes a classical droop controller.

IV. Operation Principle

This section firstly describes the operation modes of each individual DER converter. Then, the concept is extended at the microgrid level.

A. Operation modes of each individual DER

From the standpoint of each individual DER converter, the operation modes can be classified into *power regulation mode* and *bus regulation mode*.

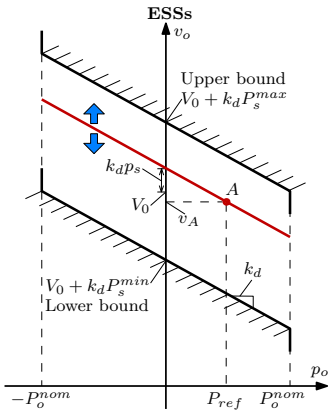

Figure 3. Operation principle of ESSs in power regulation mode.

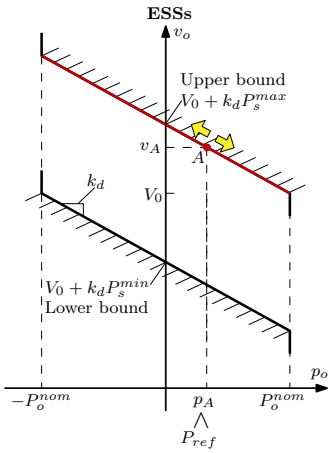

Figure 4. Operation principle of ESSs in bus regulation mode.

1) Power regulation mode: in power regulation mode, a generic DER exchanges the desired power P_{ref} with the dc microgrid while the GI converter regulates the bus voltage. ESSs are charged or discharged according to the desired targets and DGs perform MPPT. For example, Fig. 3 shows the operation principle of one ESS converter in power regulation mode. Let us assume that the bus voltage is regulated at v_A, being v_A not necessarily equal to V_0. To achieve power flow control, the droop curve of the ESS controller is shifted upwards or downwards by $k_d \cdot p_s$ produced by the power regulator $G_p(s)$. Then, the offset $k_d \cdot p_s$ is added to the voltage set point V_0, forcing the converter to operate at point A and to have an output p_o that matches the power reference P_{ref}. Correspondingly, if the bus voltage stands at V_0, p_s is equal to P_{ref}.

2) Bus regulation mode: in bus regulation mode, DER converters take responsibility of regulating bus voltage. In this case, the output power p_o depends on load power absorption and it is not equal, in general, to the given power reference P_{ref}. If p_o is larger than P_{ref}, the power loop controller saturates p_s at its lower level P_s^{min} and the droop curve lays at its lower bound. Conversely, if p_o is smaller than P_{ref}, p_s reaches its higher level P_s^{max} and the droop curve lays at its upper bound, as depicted in Fig. 4. The operation point of the ESS converter stays within the lower and upper bound in a way that depends on the specific loading conditions. This behavior is similar to the conventional droop control.

3) Transition mechanism: seamless transition between power regulation mode and bus regulation mode is one important feature of the proposed controller. Here we take the following example to explain the principle of transition. An ESS converter switches from power regulation mode to bus regulation mode when the GI converter stops transmitting power from the upstream grid to the microgrid. This process can be divided into three stages, as presented in Fig. 5.

Stage 1: the original operation point of the ESS converter is $A(V_0, P_{ref})$. After losing the support from GI converter, the power balance within the microgrid is not ensured. The bus voltage starts to decrease due to the power deficiency. As droop loop responds faster than power loop, the effect of power loop can be neglected. According to the control scheme, the following equation can be derived:

$$\Delta v_o \approx \Delta v_{ref} = -k_d \cdot \Delta p_m + k_d \cdot \Delta p_s \approx -k_d \cdot \Delta p_m \qquad (2)$$

where v_o is the output voltage of the ESS converter, v_{ref} is the reference of output voltage, p_s is the output of power regulator $G_p(s)$. As can be seen, the droop loop has a major role on bus voltage. Consequently, the operation point of the ESS converter slides from A to B along the droop curve. As a result, the ESS converter increases its output power to compensate the power shortage. Therefore, the change rate of p_s increases because the difference between output power p_o and power reference P_{ref} increases.

Stage 2: once p_s changes at the same pace as v_o, the transition process steps into the second stage:

$$\Delta v_o = k_d \cdot \Delta p_s \qquad (3)$$

Then, due to the effect of the power controller, bus voltage deviates together with the droop curve. The operation point of the ESS converter moves from B to C and p_o remains unchanged in this stage.

Stage 3: the third stage begins when p_s hits its lower bound P_s^{min}. In this stage:

$$\Delta p_s = 0 \qquad (4)$$

Droop curve reaches its lower bound and the power controller is inhibited. The bus voltage is then determined again by the droop controller; and it continues to decrease until p_o meets the load power demand. Finally, the operation point of the ESS converter reaches D and the microgrid enters another steady state operating point.

B. Operation modes of microgrid

The following three modes of operation are explored for microgrids adopting the proposed control method:

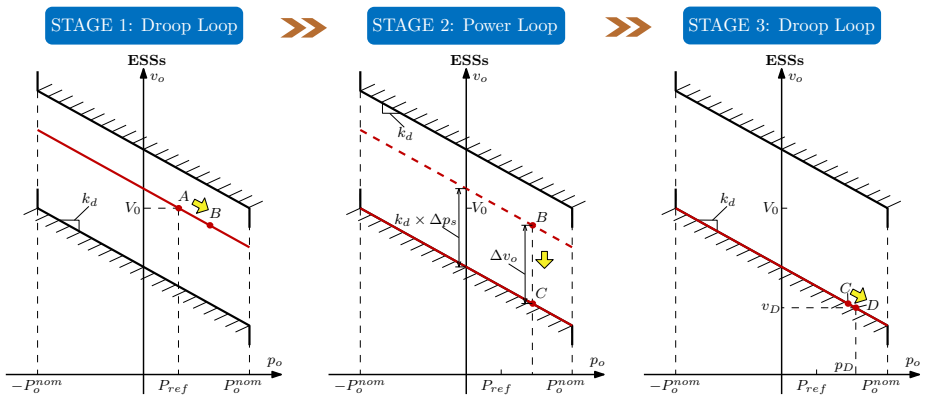

Figure 5. Transition from power regulation mode to bus regulation mode.

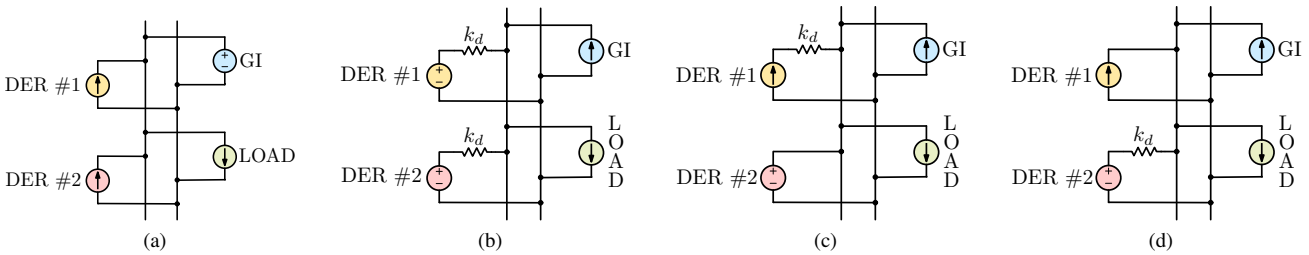

Figure 6. Equivalent models of dc microgrid in different operation conditions. (a) in mode I; (b) in mode II, situation 1; (c) in mode II, situation 2; (d) in mode II, situation 3.

1) MODE I: in this mode, the GI converter compensates the power surplus or deficit within the microgrid through its connection with the upstream grid and maintains the bus voltage at V_0. The DERs converters operate in power regulation mode, tracking their own power reference P_{ref}. The equivalent microgrid model is shown in Fig. 6a.

2) MODE II: this mode occurs when the GI converter is incapable of controlling the bus voltage. There are two possible causes for this mode: the upstream ac grid is unavailable or the required power flow exceeds the GI converter ratings. In these cases, the output power of the GI converter is limited to its nominal value or to zero, which means that the GI converter turns into a power source. DERs converters are unaware of this situation, and they are automatically reconfigured so that at least one converter operates in bus regulation mode, while the others operate in power regulation mode.

A dc microgrid including two DERs converters is here considered for the purpose of explanation. The only difference between these two converters is their power references: $P_{ref_1} > P_{ref_2}$.

- Situation 1: Converter #1 and #2 are in bus regulation mode. Both of the droop curves of the two converters are saturated at the upper bound, if:

$$P_{ref_1} > P_{ref_2} > \frac{P_L}{2} \tag{5}$$

where P_L is the load power. Or they are saturated at the lower bound, if:

$$\frac{P_L}{2} > P_{ref_1} > P_{ref_2} \tag{6}$$

In this situation, these two converters share the load equally. The equivalent microgrid model in this case is shown in Fig. 6b.

- Situation 2: Converter #1 is in bus regulation mode while converter #2 is in power regulation mode. Converter #2 tracks its power reference P_{ref_2} and converter #1 supplies the remaining power demand, that is, $P_L - P_{ref_2}$. The droop curve for converter #1 is saturated at the upper bound in this situation. The condition for this situation is:

$$P_{ref_1} > \frac{P_L}{2} > P_{ref_2} \quad \& \quad P_{ref_1} + P_{ref_2} > P_L \tag{7}$$

The equivalent microgrid model in this case is shown in Fig. 6c. Equal load distribution is not obtained.

- Situation 3: Converter #1 is in power regulation mode while converter #2 is in bus regulation mode. Similar to situation 2, the droop curve for converter #2 is saturated at the lower bound. The relationship between P_{ref_1}, P_{ref_2} and P_L can be expressed as:

$$P_{ref_1} > \frac{P_L}{2} > P_{ref_2} \quad \& \quad P_{ref_1} + P_{ref_2} < P_L \tag{8}$$

The equivalent microgrid model in this case is shown in Fig. 6d.

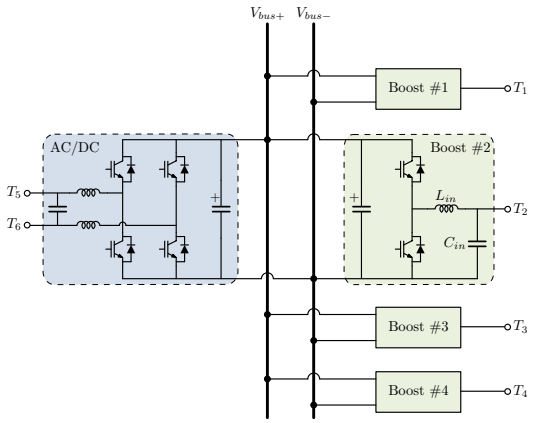

Figure 7. Schematic of the experimental testbed.

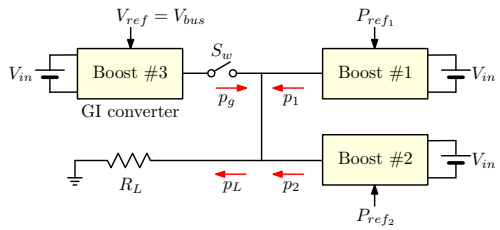

Figure 8. The case studied.

Fortunately, this uncontrolled mode does not takes a long period (e.g., several seconds) and ends when the next communication starts.

3) MODE III: this mode refers to the case in which DERs converters are aware that the GI converter is in abnormal operation. Appropriate power references are chosen for DERs converters, to guarantee that these converters operate in a predefined way. How to select power references in this mode falls outside the scope of the paper.

V. Experimental results

The experimental testbed is constituted of one full-bridge rectifier and four boost converters, as illustrated in Fig. 7.

To evaluate the proposed control method, the microgrid of Fig. 8 is considered. The GI single-phase rectifier is substituted by the boost converter #3 to avoid the second-order ripple on bus voltage, whose effects are currently under investigation. Moreover, the simplified configuration of Fig. 8 also covers the case where the GI is equipped by a second stage dc-dc converter as in [5] .The proposed controller is applied to two boost converters #1 and #2. System parameters are reported in Table. I.

A. Test in power regulation mode

In mode I converter #1 and #2 operate in power regulation mode. A step change from $0\,\mathrm{kW}$ to $1.6\,\mathrm{kW}$ is applied to P_{ref_2}. The resulting transient response is displayed in Fig. 9. p_2 rises smoothly from $0\,\mathrm{kW}$ to $1.6\,\mathrm{kW}$, with a settling time of about $100\,\mathrm{ms}$. Consequently, p_g reduces to $1.6\,\mathrm{kW}$ to maintain the power balance.

Table I
System Parameters

Parameter	Symbol	Value
Converters		
Input voltage	V_{in}	$200\,\mathrm{V}$
Nominal bus voltage	V_{bus}	$380\,\mathrm{V}$
Nominal power	P_o^{nom}	$5\,\mathrm{kW}$
Input side inductance	L_{in}	$1.6\,\mathrm{mH}$
Input side capacitance	C_{in}	$50\,\mu\mathrm{F}$
Total bus capacitance	C_{dc}	$2.2\,\mathrm{mF}$
Switching frequency	f_{sw}	$12.5\,\mathrm{kHz}$
Load Resistance	R_L	$250\,\Omega$
Droop Loop		
Voltage set point	V_0	$380\,\mathrm{V}$
Droop coefficient	k_d	$2\,\mathrm{V/kW}$
Cutoff frequency of low pass filter	ω_c	$2\pi \cdot 15\,\mathrm{rad/s}$
Power Loop		
Upper saturation level	P_s^{max}	$5\,\mathrm{kW}$
Lower saturation level	P_s^{min}	$-5\,\mathrm{kW}$

B. Test of transition from power regulation to bus regulation mode

Fig. 10 shows the transition from power regulation mode to bus regulation mode. This event is triggered by opening the switch S_w. In stage 1, bus voltage rises quickly to $383\,\mathrm{V}$. At the same time, p_1 and p_2 decrease to $350\,\mathrm{W}$, which is close to the power in steady state. In stage 2, due to the power controller, bus voltage increases linearly and p_1 and p_2 remain constant. In stage 3, for converter #1 and #2, droop curves are fixed at their upper bounds and the operation points change slightly to steady state, where bus voltage equals $390\,\mathrm{V}$, p_1 and p_2 equal $300\,\mathrm{W}$. Finally, the microgrid operates in mode II, situation 1. Consistent with the theoretical analysis, a smooth transition is achieved.

C. Test in bus regulation mode

In this test, converters #1 and #2 operate in bus regulation mode. The load resistance steps down from $250\,\Omega$ to $70\,\Omega$. The total load power increases to $1500\,\mathrm{W}$ and each converter outputs $750\,\mathrm{W}$ more. As a result, bus voltage decreases by $1.5\,\mathrm{V}$.

VI. Conclusion

This paper presents a power-based controller for DERs in dc microgrid. The controller operates in power regulation mode and bus regulation mode, to regulate output power and bus voltage respectively. The seamless transition mechanism between these two modes is also ensured. After the disconnection of the upstream grid, the microgrid operates in different situations according to the relationship between P_{ref} of DERs and load. The tests of tracking power reference step, transiting from power regulation to bus regulation mode, and reacting to

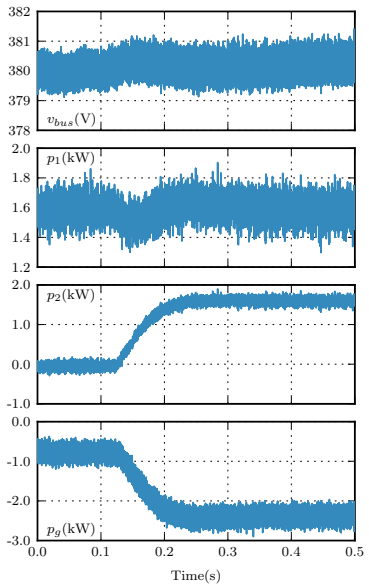

Figure 9. Test of power regulation mode. $P_{ref_1} = 1.6\,\text{kW}$

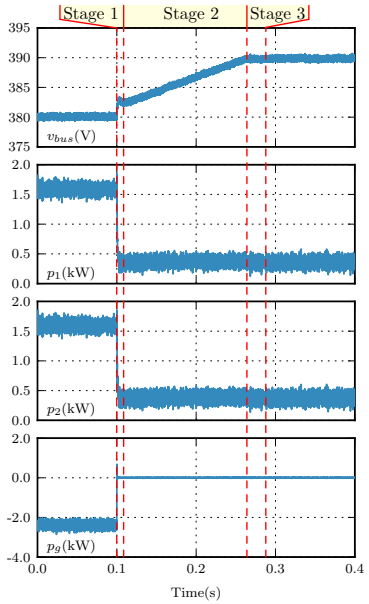

Figure 10. Test of transition from power regulation to bus regulation mode. $P_{ref_1} = P_{ref_2} = 1.6\,\text{kW}$

load step have been experimentally verified on a small-scale dc microgrid testbed.

REFERENCES

[1] R. H. Lasseter, "Smart distribution: Coupled microgrids," *Proceedings of the IEEE*, vol. 99, no. 6, pp. 1074–1082, June 2011.

[2] T. Dragicevic, J. C. Vasquez, J. M. Guerrero, and D. Skrlec, "Advanced lvdc electrical power architectures and microgrids: A step toward a new generation of power distribution networks." *IEEE Electrification Magazine*, vol. 2, no. 1, pp. 54–65, March 2014.

[3] K. Sun, L. Zhang, Y. Xing, and J. M. Guerrero, "A distributed control strategy based on dc bus signaling for modular photovoltaic generation systems with battery energy storage," *IEEE Transactions on Power Electronics*, vol. 26, no. 10, pp. 3032–3045, Oct 2011.

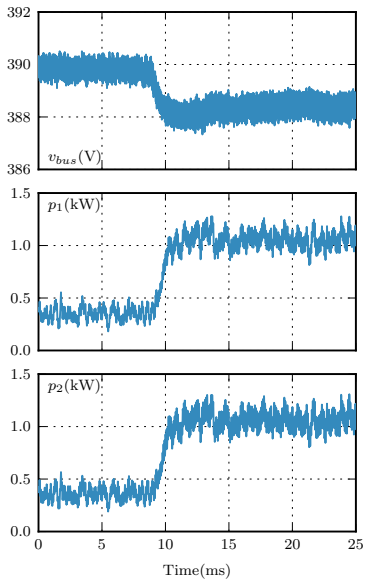

Figure 11. Test of bus regulation mode. $P_{ref_1} = P_{ref_2} = 1.6\,\text{kW}$

[4] J. Schonbergerschonberger, R. Duke, and S. D. Round, "Dc-bus signaling: A distributed control strategy for a hybrid renewable nanogrid," *IEEE Transactions on Industrial Electronics*, vol. 53, no. 5, pp. 1453–1460, Oct 2006.

[5] I. Cvetkovic, D. Dong, W. Zhang, L. Jiang, D. Boroyevich, F. C. Lee, and P. Mattavelli, "A testbed for experimental validation of a low-voltage dc nanogrid for buildings," in *2012 15th International Power Electronics and Motion Control Conference (EPE/PEMC)*, Sept 2012, pp. LS7c.5–1–LS7c.5–8.

[6] F. Chen, R. Burgos, D. Boroyevich, and W. Zhang, "A nonlinear droop method to improve voltage regulation and load sharing in dc systems," in *2015 IEEE First International Conference on DC Microgrids (ICDCM)*, June 2015, pp. 45–50.

[7] S. Anand, B. G. Fernandes, and J. Guerrero, "Distributed control to ensure proportional load sharing and improve voltage regulation in low-voltage dc microgrids," *IEEE Transactions on Power Electronics*, vol. 28, no. 4, pp. 1900–1913, April 2013.

[8] X. Lu, J. M. Guerrero, K. Sun, and J. C. Vasquez, "An improved droop control method for dc microgrids based on low bandwidth communication with dc bus voltage restoration and enhanced current sharing accuracy," *IEEE Transactions on Power Electronics*, vol. 29, no. 4, pp. 1800–1812, April 2014.

[9] Y. Gu, W. Li, and X. He, "Frequency-coordinating virtual impedance for autonomous power management of dc microgrid," *IEEE Transactions on Power Electronics*, vol. 30, no. 4, pp. 2328–2337, April 2015.

[10] Q. Xu, X. Hu, P. Wang, J. Xiao, P. Tu, C. Wen, and M. Y. Lee, "A decentralized dynamic power sharing strategy for hybrid energy storage system in autonomous dc microgrid," *IEEE Transactions on Industrial Electronics*, vol. PP, no. 99, pp. 1–1, 2016.

[11] X. Lu, K. Sun, J. M. Guerrero, J. C. Vasquez, and L. Huang, "State-of-charge balance using adaptive droop control for distributed energy storage systems in dc microgrid applications," *IEEE Transactions on Industrial Electronics*, vol. 61, no. 6, pp. 2804–2815, June 2014.

[12] X. Zhao, Y. W. Li, H. Tian, and X. Wu, "Energy management strategy of multiple supercapacitors in a dc microgrid using adaptive virtual impedance," *IEEE Journal of Emerging and Selected Topics in Power Electronics*, vol. 4, no. 4, pp. 1174–1185, Dec 2016.

[13] S. Lissandron and P. Mattavelli, "A controller for the smooth transition from grid-connected to autonomous operation mode," in *2014 IEEE Energy Conversion Congress and Exposition (ECCE)*, Sept 2014, pp. 4298–4305.

[14] L. Xu and D. Chen, "Control and operation of a dc microgrid with variable generation and energy storage," *IEEE Transactions on Power Delivery*, vol. 26, no. 4, pp. 2513–2522, Oct 2011.